Materials Science Forum
ISSN: 1662-9752, Vol. 1028, pp 269-275

Submitted: 2020-11-11
Revised: 2020-12-10
Accepted: 2020-12-19
Online: 2021-04-29

Crystal Characterization of Anionic Salt Compounds as Composite of Solid Propellant Oxidizing Agent

Sovian Aritonang[1,a], Maykel Manawan[1,b*], Mas Ayu E. H[1,c], Timbul Siahaan[1], Shofi Muktiana S.[1], Hanung Bayu Setiawan[1], Sih Wuri Andayani[2], Gaos Abdul Karim[2], Alfiz Muhammad Qizwini[2], Otong Nurhilal[3], Togar Saragi[3], Risdiana[3]

[1]Faculty of Defense Technology, Indonesia Defense University, Bogor 16810, Indonesia

[2]Center for Material and Technical Product, Bandung 40135, Indonesia

[3]Department of Physics, Universitas Padjadjaran, Sumedang 45363, Indonesia

[a]Sovian.aritonang@idu.ac.id, [b]maykel.manawan@idu.ac.id (corresponding authors), [c]ayu.hafizah@idu.ac.id, [d]timbul.siahaan@idu.ac.id, [e]shofi.mkbr@ts.idu.ac.id, [f]hanung.setiawan@tp.idu.ac.id, [g]andayani@kemenperin.go.id, [h]gaos@, [i]alfiz@, [j]risdiana@phys.unpad.ac.id

Keywords: Inorganic compound, solid based propellant, oxidizer, x-ray diffraction, Rietveld refinement, electrostatic potential energy

Abstract. Composite solid propellants are preferred for use in defense and space applications because of their high energy density and simplicity. Oxidizers take up the highest percentage in propellant ingredient. KNO_3, $KClO_4$ and $K_2Cr_2O_7$ are among the inorganic oxidizers with similar cation for present study, and their chemical and physical properties are fully understood. However, the relationship between thermal stability and electrostatic potential energy based on structural analysis has not yet been studied. In this study we used high resolution XRD data to study the electrostatic potential energy of the KNO_3, $KClO_4$ and $K_2Cr_2O_7$ crystal structures.

Introduction

Solid propellants are most preferred than liquid or gas propellants due to easier to store and to handle. Solid propellants have high energy density, therefore produce a high temperature of combustion and high propulsive force. That characteristics make solid propellant ideal for military applications as well as space shuttle and many other orbital launch vehicles [1,2]. A solid propellant consists of several chemical ingredients such as oxidizer (60-80%), fuel (maximum 25%), binder, plasticizer, curing agent, stabilizer, and cross-linking agent. The specific chemical composition depends on the desired combustion characteristics for a particular mission [1-5]. The oxidizer classified as inorganic and organic based compounds.

Potassium nitrate (KNO_3), potassium perchlorate ($KClO_4$) and potassium dichromate ($K_2Cr_2O_7$) are among inorganic oxidizer that selected in this study due to the similar cation (K^{1+}), but with different anion (NO_3^{1-}, ClO_4^{1-}, $Cr_2O_7^{1-}$) [4-9]. Different anions give a different chemical reaction to produce a different deflagration and detonation, which is important property of propellant. The chemical reaction rate is depending on the chemical bonding between the atom inside the structure [10].

To understand the chemical bond and the electronic structure of ionic crystals, estimation of electrostatic potentials in the periodic arrangement of the ions is an inevitable task. There are numbers of methods are used to calculate electrostatic potential energy [11-13], and Fourier methods were chosen due to it fast computing time and use the input from Rietveld refinement result [14,15].

This report presents the results of a preliminary study of KNO_3, $KClO_4$ and $K_2Cr_2O_7$ with X-ray diffraction to determine the electrostatic potential energy based on the Rietveld refinement results.

Experimental Method

Material classification were used in this research have high quality grade under pro analysis classification from Merck. Potassium Dichromate ($K_2Cr_2O_7$) was used had purity minimum 99.98%. While Potassium Nitrate (KNO_3) and Potassium Perchlorate ($KClO_4$) have purity ≥ 99 %. The third chemical agents are classified as inorganic oxidizing agents, powder based and stable at room temperature under dry based condition. 3 gr sample of each compound were grinded and sieved to get homogeneous particle size smaller than 75 microns. Fine powder than prepared in circular PMMA holder with inner diameter of 25 mm and depth of 2 mm. To prevent the preferred orientation effect, a rotation sample stage is used with speed of 15 rotation per minutes.

XRD data were obtained on a Bruker D8 Advance diffractometer with Cu X-ray anode operate at 1.6 kW (40 kV, 40 mA), line focus of 0.04 x 8 mm, arm radius of 250 mm (primary and secondary), divergence slit of 1°, soller slit of 2.5° (primary and secondary) and LYNXEYE-XET position-sensitive detector (PSD) without *K*β filter.

Data acquisition were collected at 2θ range of 10° - 100°, with step size of 0.02° 2θ (4500 data points) and scan speed of 1 second per data. Suppose for scintillation counter detector (0-D detector), total acquisition time about 4500 seconds or 1.25 hours, but due to the advantage of LYNXEYE-XET PSD (1-D detector), the total acquisition time reduced to about 8 minutes for each sample.

The Rietveld refinement were performed with Bruker-Topas version 6 implemented with convolution-based profile fitting / fundamental parameters approach which provides high accuracy and precision in determining lattices and structure parameters [16-19].

Result and Discussion

The raw data and the result of the Rietveld refinement of KNO_3, $KClO_4$ and $K_2Cr_2O_7$ in Fig. 1 shows a good agreement between experimental data and simulated pattern from ICDD reference database PDF 01-071-1558 (orthorombic Pmcn), PDF 04-007-6710 (Orthorombic Pnma) and PDF 04-015-3612 (Triclinic P-1), respectively.

The highest quality of data was indicated by peak to background ratio beter than 200 for all diffractograms resulted a smaller expected R-factor (Rexp); 3.88, 5.52 and 5.90 for KNO_3, $KClO_4$ and $K_2Cr_2O_7$, respectively. The indicator for a good Rietveld refinement, weighted R-factor (Rwp), are close to Rexp results a small Godness of Fit (GoF); 1.18, 1.17 and 1.05 for KNO_3, $KClO_4$ and $K_2Cr_2O_7$, respectively. Due to this high quality of data, precise lattice parameters, atomic position and thermal displacement parameters are able to determine. The complite summary of all refined parameters are listed on Table 1 and Table 2.

Fig 2 shows the represent 3D structures of KNO_3, $KClO_4$ and $K_2Cr_2O_7$ from Rietveld refinement. The N^{5+} in KNO_3 has plane like coordination with three O^{2-}, while Cl^{7+} in $KClO_4$ and Cr^{6+} in $K_2Cr_2O_7$ has tetrahedral coordination with four O^{2-}. K^{1+} act as buffer for all the structures. While the polyhedral with the center atom of N^{5+} and Cl^{7+} in KNO_3 and $KClO_4$ are stand alone, there are two pairs of Cr^{6+} in $K_2Cr_2O_7$ was connected by two O^{2-} denotes O4 and O11. The share of O^{2-} ion among Cr^{6+} causes Cr–O4 and Cr–O11 bond to streches and create a distorted polyhedra.

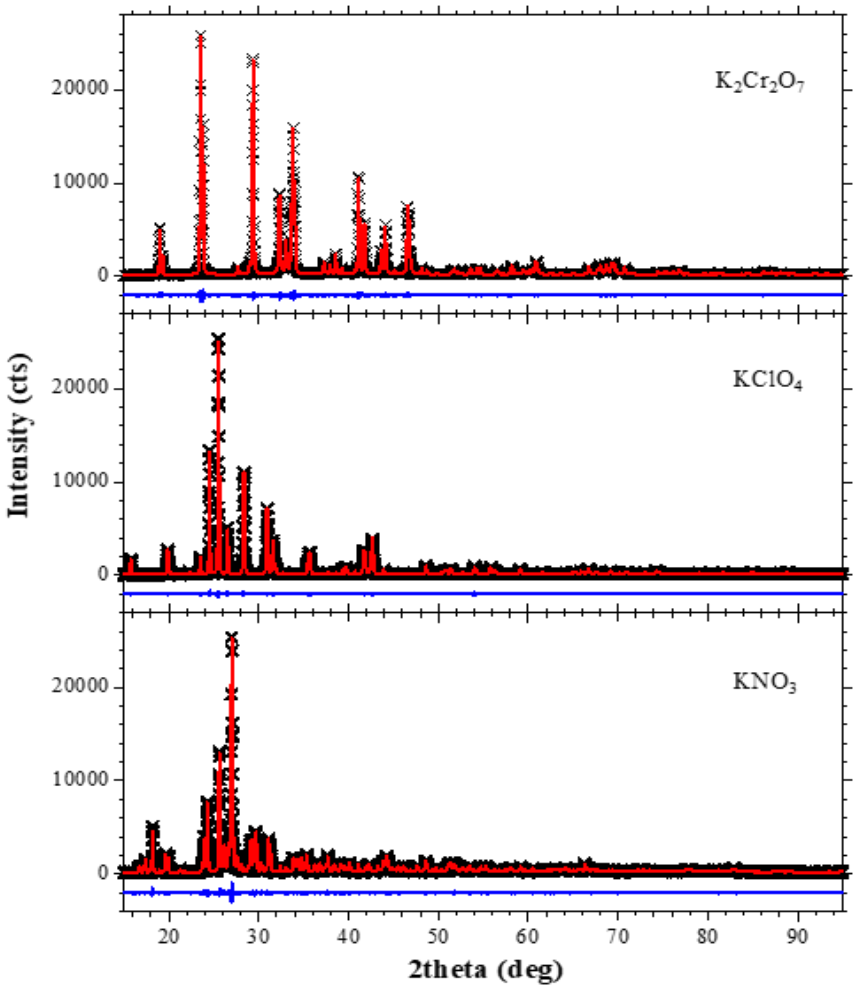

Figure 1. Rietveld refinement of KNO_3, $KClO_4$ and $K_2Cr_2O_7$ (Color online: black – data, red – model, blue – residual).

Table 1. Summary of refined lattice parameters and figure of merits.

		KNO_3	$KClO_4$	$K_2Cr_2O_7$
Space Group		Pmcn	Pnma	P-1
Cell Mass		404.413(0)	554.196(0)	1176.738(8)
Cell Volume (Å^3)		319.375(1)	363.753(1)	726.881(6)
Crystal Density (g/cm^3)		2.103(0)	2.530(0)	2.686(1)
Crystallite size (nm)		361(5)	636(6)	170(2)
Strain		0.00025(4)	0.00042(1)	0.00011(0)
Lattice Parameters	*a* (Å)	5.41592(9)	8.85524(1)	7.38581(8)
	b (Å)	9.16965(7)	5.66352(1)	7.46347(0)
	c (Å)	6.43132(7)	7.25477(1)	13.40167(5)
	Alpha (°)	90	90	96.18341(9)
	Beta (°)	90	90	98.05732(8)
	Gamma (°)	90	90	90.87155(4)
Rexp		3.88	5.52	5.90
Rwp		4.58	6.47	6.18
GoF		1.18	1.17	1.05
Refined parameters		21	19	31

Table 2. Summary of refined structure parameters.

	x	y	z	Occupancy	Uiso	Multiplicity	Wyckoff
KNO_3 atomic parameters							
K	0.25	0.4166	0.7568	1	2.3950	4	c
N	0.25	0.7548	0.9152	1	2.1213	4	c
O1	0.25	0.8902	0.9107	1	3.1767	4	c
O2	0.4492	0.6866	0.9151	1	3.0556	8	d
$KClO_4$ atomic parameters							
K	0.1809	0.25	0.3374	1	1.4480	4	c
Cl	0.0679	0.25	0.8105	1	1.2645	4	c
O1	0.1885	0.25	0.9419	1	1.3355	4	c
O2	0.4197	0.5438	0.1952	1	1.0175	8	d
O3	0.4253	0.25	0.5981	1	3.2709	4	c
$K_2Cr_2O_7$ atomic parameters							
K1	1.1034	0.6692	0.6403	1	1.5223	2	i
K2	0.2501	0.7671	0.3496	1	1.4820	2	i
K3	0.6624	-0.0853	0.1584	1	1.4915	2	i
K4	0.6949	0.6522	-0.1358	1	1.4512	2	i
Cr1	0.5917	0.7688	0.6072	1	2.4453	2	i
Cr2	0.7929	0.8068	0.4137	1	2.2866	2	i
Cr3	0.8170	0.4257	0.1136	1	1.9518	2	i
Cr4	0.8133	0.1524	-0.0831	1	2.4982	2	i
O1	0.7196	0.6125	0.6490	1	2.7066	2	i
O2	0.5547	0.9100	0.7017	1	2.7745	2	i
O3	0.4024	0.6852	0.5451	1	2.8274	2	i
O4	0.7076	0.8928	0.5268	1	2.3774	2	i
O5	0.9591	0.6753	0.4429	1	2.2858	2	i
O6	0.8688	0.9716	0.3608	1	2.5661	2	i
O7	0.6344	0.6951	0.3365	1	2.8322	2	i
O8	0.6890	0.2929	0.1638	1	2.3695	2	i
O9	0.9756	0.5180	0.2000	1	2.3774	2	i
O10	0.6949	0.5755	0.0612	1	2.6869	2	i
O11	0.9293	0.2959	0.0227	1	1.9258	2	i
O12	0.6919	-0.0003	-0.0433	1	2.3205	2	i
O13	0.9604	0.0612	-0.1486	1	2.8701	2	i
O14	0.6774	0.2736	-0.1518	1	2.1721	2	i

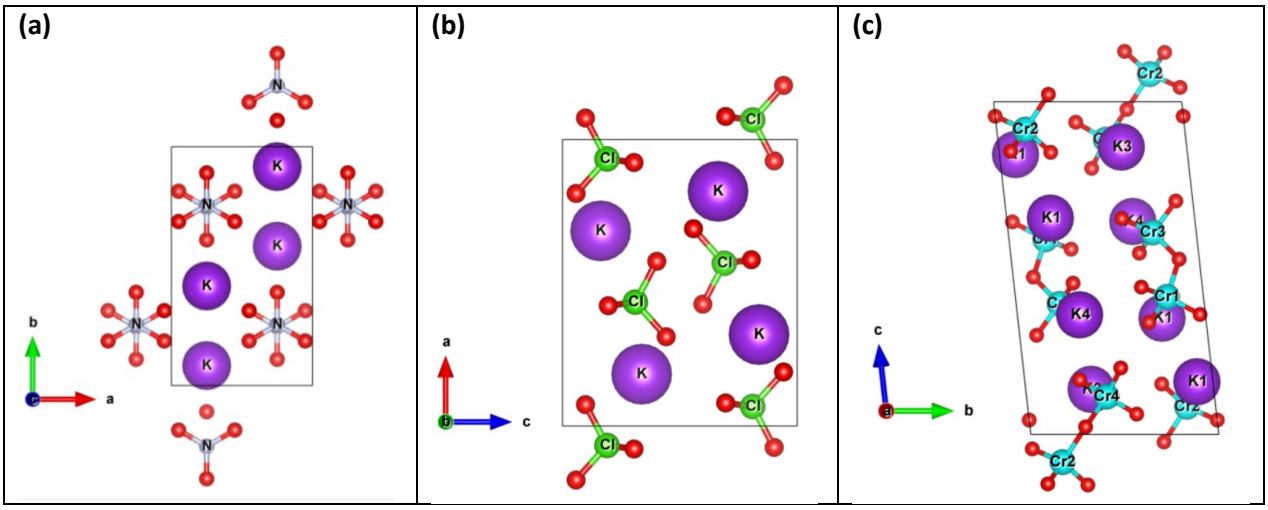

Figure 2. Refined crystal structure model of (a) KNO_3, (b) $KClO_4$ and (c) $K_2Cr_2O_7$.

The formal atomic charges (K = +1, N = +5, Cl = +7, Cr = +6, O = -2) need to add into the Crystallographic Information File (CIF) in order determine the bond valence parameter, further calculate the electrostatic potential energy.

Information concerning the oxidation state of the elements was determined by bond-valence sum, *BVS*, using the Brown's model as shown in Eq. 1 [20,21].

$$BVS = \sum_{i=1}^{n} \exp\left(\frac{r_0 - r_i}{B}\right) \quad (1)$$

where $B = 0.37$, and $r_0 = 2.113$ Å for K−O pair, $r_0 = 1.361$ Å for N−O, $r_0 = 1.669$ Å for Cl−O and $r_0 = 1.794$ Å for Cr−O from Brese et al. [22], and r_i (polyhedral ionic radii) are taken from Shanon et al. [23]. As suggested, N, Cl and Cr are five-valent, seven-valent, and six-valent, respectively.

The electrostatic energy is calculated from new CIF files where the atomic charges are taken from *BVS* calculation. The electrostatic potential, ϕ_i, for site i is computed by using Eq. 2 [14, 24].

$$\phi_i = \sum_j \frac{Z_j}{4\pi\epsilon_0 l_{ij}} \quad (2)$$

where Z_j is the oxidation state of the j^{th} ion in the unit of the elementary charge e (1.602177×10^{-19} C), ϵ_0 is the vacuum permittivity (8.854188×10^{-12} Fm^{-1}), and l_{ij} is the distance between ions i and j in the crystal. Electrostatic potential or Madelung energy, E_M, per asymmetric unit is calculated by using the formula as shown in Eq. 3 [14,24].

$$E_M = \frac{1}{2}\sum_i \phi_i Z_i W_i \quad (3)$$

with $$W_i = \frac{(occupancy)\times(number\ of\ equivalent\ positions)}{(number\ of\ general\ equivalent\ positions)}$$

Table 3 shows the calculated bond valence sum for each atom and electrostatic energy per asymmetric unit for KNO_3, $KClO_4$ and $K_2Cr_2O_7$.

Table 3. *BVS* and E_M per asymmetric unit.

	KNO_3			$KClO_4$			$K2Cr_2O_7$		
	K	N	O	K	Cl	O	K	Cr	O
BVS	1.275	4.992	1.652 *	1.086	7.535	-1.632*	1.023	5.927*	1.652 *
E_M (MJ/mol)		-13.16(8)			-17.76(2)			-92.82(8)	

*More than one atom, value is based on average

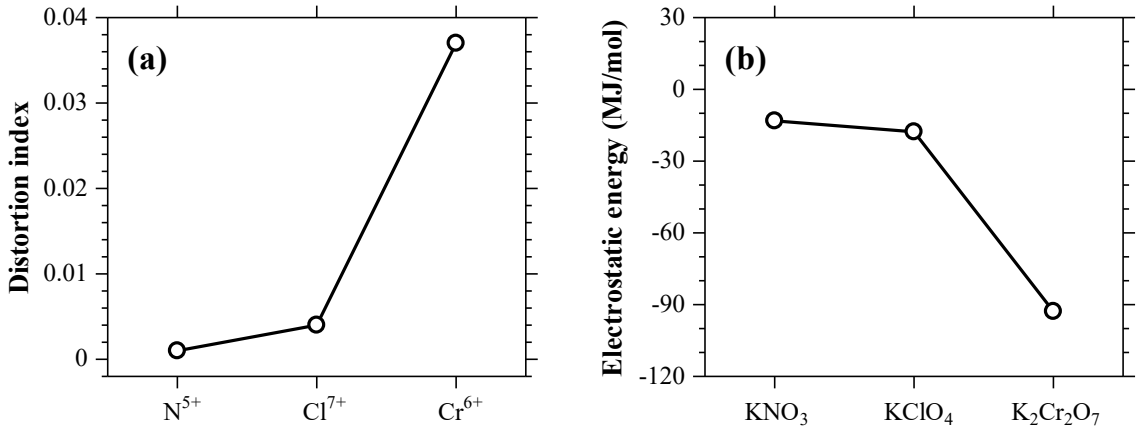

Figure 3. (a) Distortion index and (b) Electrostatic energy per asymmetric unit.

Fig. 3(a) shows the polyhedral distortion index according to the coordination complex with O^2 and electrostatic energy per asymmetric unit (Fig. 3(b)). It is clearly be seen that the degree of distortion from the centre of polyhedral are increase with the coordination numbers, as well as the complexity with the decrease of structural symmetry. The same pattern also shows in electrostatic energy but in opposite trend that shows an increase in bond energy which concluded that $K_2Cr_2O_7$ has the most potential energy compared to KNO_3 and $KClO_4$.

Conclusions

The crystallography analysis on KNO_3, $KClO_4$ and $K_2Cr_2O_7$ has been studied with powder X-ray diffraction. Rietveld refinement are successfully performed and the related parameters to the propellants energy performance are successfully determined. The electrostatic energy per asymmetric unit for KNO_3, $KClO_4$ and $K_2Cr_2O_7$ are -13.16(8) MJ/mol, -17.76(2) Mj/mol and - 92.82(8) MJ/mol, respectively. The $K_2Cr_2O_7$ has the most potential energy compared to KNO_3 and $KClO_4$.

Acknowledgment

The authors gratefully acknowledge for the financial support provided by the Directorate of Research and Community Service Universitas Pertahanan Indonesia under program Grants of Research LPPM UNHAN 2020 contract No. 39/VII/2020/FTP. We are also thankful for the support from Balai Besar Bahan dan Barang Teknik (B4T) and IPB XRD Forum

References

[1] S. Chaturvedi, P.N. Dave, Solid propellants: AP/HTPB composite propellants, Arab. J. Chem 12 (2019) 2061-2068. doi.org/10.1016/j.arabjc.2014.12.033.

[2] M.W. Beckstead, K. Puduppakkam, P. Thakre, V. Yang, Modeling of combustion and ignition of solid-propellant ingredients, Prog. Energy Combust. Sci. 33 (2007) 497-551. doi.org/10.1016/j.pecs.2007.02.003.

[3] N. Yadav, P.K. Srivastava, M. Varma, Recent advances in catalytic combustion of AP-based composite solid propellants, Def. Tech. xxx, (2020) xxx-xxx. In Press, Corrected Proof. doi.org/10.1016/j.dt.2020.06.007

[4] K. Kishore, K. Shridhara, Solid propellant chemistry, condensed phase behavior of ammonium perchlorate based solid propellants, Defence Research Development Organization, and Ministry of Defence, New Delhi, India, 1999

[5] K. Kishore, M.R. Sunitha, Effect of transition metal oxides on decomposition and deflagration on composite solid propellant systems: a survey. AIAA J 17 (1979) 1118-1125. doi.org/10.2514/3.61286

[6] R. Baldissera, M. Poletto, Solid propellants for rockets: a methodology to obtain high purity KNO_3 from an inexpensive source, Int. J. Res. Eng. Technol. 7 (2018) 52-56. doi.org/10.15623/ijret.2018.0709007
[7] S.J. Mehilal, P.O. Singh, B.Bhattacharya, Evaluation of Potassium Perchlorate as a Burning Rate Modifier in Composite Propellant Formulations, Cent. Eur. J. Energetic Mater 13 (2016) 231-245. doi.org/10.22211/CEJEM/64980
[8] V.P. Sinditskii, V. Y. Egorshev, Combustion mechanism of ammonium-nitrate-based -propellants, J. Propuls. Power 24 (2008) 1068-1078. doi.org/10.2514/1.35233
[9] F. Maggi, L. Arosio, L. Galfetti, Catalyst screening for ammonium nitrate oxidizer, 7th European Conference for Aero Space Sciences (2017) 1-9. doi.org/10.13009/EUCASS2017-520
[10] R. Meyer, J. Kvhler, A. Homburg, Explosives, 5th Ed., Wiley VCH, Weinheim, 2002.
[11] E.I. Izgorodina, U.L. Bernard, P.M. Dean, J.M. Pringle, D.R. MacFarlane, The Madelung constant of organic salts, Cryst. Growth Des. 9 (2009) 4834-4839. doi.org/10.1021/cg900656z
[12] G. Vaman, The electrostatic potential of a periodic lattice, Rep. Math. Phys. 75 (2015) 135-147. doi.org/10.1016/S0034-4877(15)60029-5
[13] D. Nguyen, P. Macchi, A. Volkov, Fast analytical evaluation of intermolecular electrostatic interaction energies using the pseudoatom representation of the electron density. III. Application to crystal structures via the Ewald and direct summation methods, Acta Cryst. A76 (2020) 630-651. doi.org/10.1107/S2053273320009584
[14] Izumi, F, Structure Analysis by Powder Diffraction with the RIETAN-FP-VENUS System and External Programs —1. The RIETAN-FP-VENUS System and Integrated Assistance Environment—. Materia Japan 56 (2017) 393-396. doi.org/10.2320/materia.56.393
[15] Momma, K. and Izumi, F, VESTA 3 for three-dimensional visualization of crystal, volumetric and morphology data. J. Appl. Cryst., 44 (2011) 1272-1276. doi.org/10.1107/S0021889811038970
[16] R.W. Cheary, A.A. Coelho, A fundamental parameters approach to X-ray line-profile fitting, J. Appl. Cryst. 25 (1992) 109-121. doi.org/10.1107/S0021889891010804
[17] R.W. Cheary, A.A. Coelho, J.P. Cline, Fundamental parameters line-profile fitting in laboratory diffractometers, J. Res. Natl.Inst. Stand. Tech. 109 (2004) 1-25. doi.org/10.6028/jres.109.002
[18] A. Kern, A.A. Coelho, R.W. Cheary, Diffraction Analysis of Materials: Convolution based profile fitting, Material Science, Springer, Berlin, 2004. doi.org/10.1007/978-3-662-06723-9_2
[19] A. Kern, Principle and Application of Powder Diffraction: Convolution based profile fitting, Blackwell, New Jersey, 2008. doi.org/10.6028%2Fjres.109.002
[20] I.D. Brown, D. Altermatt, Bond-valence parameters obtained from a systematic analysis of the Inorganic Crystal Structure Database, Acta Crystallogr., Sect. B: Struct. Sci., 41 (1985) 244-247. doi.org/10.1107/S0108768185002063
[21] I.D. Brown, Recent Developments in the Methods and Applications of the Bond Valence Model, Chem. Rev. 109 (2009) 6858–6919. doi.org/10.1021/cr900053k
[22] N. E. Brese and M. O'Keeffe, Bond-valence parameters for solids, Acta Cryst., Sect. B: Struct. Sci., 47 (1991) 192-197. doi.org/10.1107/S0108768190011041
[23] R.D. Shannon, Revised effective ionic radii and systematic studies of interatomic distances in halides and chalcogenides, Acta Cryst., Sect. A: Cryst. Phys., Diffr., Theor. Gen. Cryst. 32 (1976) 751−767. 10.1107/s0567739476001551
[24] D.N. Aryyriou, C.J. Howard, Evaluation of Electrostatic Potentials and Madelung Constants in Ionic Crystals by the Method of Spherically Symmetric Equivalent Charges, Aust. J. Phys., 45 (1992) 239-52. doi.org/10.1071/PH920239